

Towards a Robust Out-of-the-box Neural Network Model for Genomic Data

Zhaoyi Zhang*

Songyang Cheng*

*Department of Computer Science
University of Wisconsin-Madison
Madison, WI 53715, USA*

ZZHANG825@WISC.EDU

SCHENG72@WISC.EDU

Claudia Solís-Lemus†

*Wisconsin Institute for Discovery
and Department of Plant Pathology
University of Wisconsin-Madison
Madison, WI 53715, USA*

SOLISLEMUS@WISC.EDU

Abstract

The accurate prediction of biological features from genomic data is paramount for precision medicine, sustainable agriculture and climate change research. For decades, neural network models have been widely popular in fields like computer vision, astrophysics and targeted marketing given their prediction accuracy and their robust performance under big data settings. Yet neural network models have not made a successful transition into the medical and biological world due to the ubiquitous characteristics of biological data such as modest sample sizes, sparsity, and extreme heterogeneity. Here, we investigate the robustness, generalization potential and prediction accuracy of widely used convolutional neural network and natural language processing models with a variety of heterogeneous genomic datasets. While the perspective of a robust out-of-the-box neural network model is out of reach, we identify certain model characteristics that translate well across datasets and could serve as a baseline model for translational researchers.

Keywords: Generalization error, phenotype prediction, convolutional, natural language processing

1. Introduction

Background. The ability to accurately predict phenotypes from genomic data is one of the most coveted goals of modern-day medicine and biology. Examples abound: from precision medicine where researchers want to predict a patient’s disease susceptibility based on the genetic information (Ashley, 2015; Rost et al., 2016; Katuwal and Chen, 2016; Krittanawong et al., 2017; Lee et al., 2018; Ho et al., 2019) to prediction of antibiotic-resistant bacterial strains based on the genomes of pathogenic microbes (Fjell et al., 2009; Coelho et al., 2013; Pesesky et al., 2016; Kavvas et al., 2018; Li et al., 2018). Examples extend beyond human health into soil and plant health such as the prediction of crops yield (or plant disease

*. Joint first authors with equal contribution and randomly chosen order (reproducible script in Supplementary Material)

†. Corresponding author

susceptibility) based on soil microbiome metagenomic data (Chang et al., 2017; Bokulich et al., 2018; Carrieri et al., 2019) and the prediction of pesticide-resistant microbial strains from plant bacterial pathogen genomes (Yang and Guo, 2017; Ip et al., 2018; Maino et al., 2018; Duarte-Carvajalino et al., 2018). Our ability to anticipate outcomes from data is at our scientific core when we face human disease, environmental challenges, and climate change.

Naturally, biologists and medical researchers have turned to the machine-learning community for answers given the great success of machine-learning methods in a plethora of applications such as computer vision (Hjelmås and Low, 2001; Egmont-Petersen et al., 2002) and astrophysics (Kucuk et al., 2017; Jonas et al., 2018) to name a few.

However, the success of machine-learning methods on other fields has not been easily translated to the biological realm (Chen et al., 2019; Ekins et al., 2019; Teschendorff, 2019; Dacrema et al., 2019). Indeed, the complexity of biological omics data has hampered the adoption of machine-learning models, especially neural networks. Among the main challenges of genomic data in neural network models are 1) smaller sample sizes compared to other fields and 2) heterogeneity of training samples and testing samples.

First, despite the advance in high-throughput sequencing technologies, extracting whole genomes remains a time-consuming and expensive task when sample sizes must be in the order of thousands. In addition, data privacy and restrictions on data sharing in medical research restrict scientists’ ability to combine multiple smaller datasets into larger ones suitable for neural network modeling.

Second, more important than sample size, the weak link of deep learning in biological applications is the assumption of homogeneity between training and testing samples. This assumption is violated, for example, in microbial datasets where laboratory samples (training data) and environmentally or clinically collected samples (testing data) can be intricately heterogeneous. This data heterogeneity can cause lack of robustness and generalization errors in neural network models. Robustness is the key ingredient that is needed for neural network models to translate into medical practice and into the phenotype prediction in the agricultural or environmental field.

Main contributions. In literature, there are multiple examples of successfully fit neural network models on biological or medical genomic data (Agarwal et al., 2019; Nguyen et al., 2016; Zeng et al., 2016; Shadab et al., 2020; Trabelsi et al., 2019). However, it remains uncertain whether the proposed models could be translated to other similar datasets with comparable performance. That is, we ask whether the neural network models proposed in literature are robust across heterogeneous (but similar in nature) datasets.

In addition, we approach the existing neural network models with the mindset of a biological or medical user. A biological researcher would see the neural network model in an existing publication and then would try to apply a similar model to their own dataset. First, we explore how easy it is to replicate the analysis on existing publications. Second, by making incremental changes to the model characteristics, we gauge the effect of each model component on the overall performance.

We learn mainly three things: 1) in multiple instances, we are not able to replicate the performance in existing publications either because data is not available, code is not available, or code is corrupted, incomplete or not well-documented; 2) most of the times

the good performance of existing models does not translate to alternative datasets, yet we do encounter some model characteristics (in particular, related to convolutional neural networks) that are generally robust across datasets and that could serve as a potential baseline model – albeit with modest performance – to start the prediction process from a user perspective, and 3) we find that accurate prediction is a balancing game between underfitting and overfitting, and that small changes in the architecture can have unpredictable outcomes.

The quest for robust neural network models that could tackle the complexities of biological data (and its intrinsic heterogeneity) is imminent. Neural network models cannot be fully applicable in informed patient care, medical or agricultural framework if they cannot guarantee some level of generalization potential given that genomic data are not static but constantly evolving.

The difficulty of the prediction problem in biology or medicine is such that it would be naive to believe that there will exist an out-of-the-box model that will be fully transferable. Yet, from a user perspective, it is desirable to know if there are certain model characteristics that perform modestly under scrutiny from a variety of different datasets.

While we advise biological or medical users against using out-of-the-box strategies, we conclude from our study that simple convolutional neural networks (small number of layers) are relatively robust across genomics datasets and generally not affected by the type of data encoding or the sparsity level. Overfitting is an issue on more complex CNN models (as expected), but it is relatively controlled via regularization schemes. We also find that a general LSTM layer for embedding performed relatively well across datasets and this performance was robust to batch sizes and choice of optimizer. Finally, our work raises awareness to the importance of reproducibility and replicability. As machine-learning scientists, it is crucial to accompany our work with reproducible scripts that are relatively easy to follow by the scientific community so that our findings have an impact across fields, in particular, into the biological and medical community.

Structure of the paper. We focus on two widely used neural network models found in literature for genomic data: convolutional neural networks (Section 2.2) and natural language processing (Section 2.3). For each of these models, we explored the role of specific layers, robustness to alternative datasets, the role of data encoding, the role of the optimizer, the role of batch size, and the role of embedding size. We present our findings for convolutional neural networks in Section 3.1 and for natural language processing in Section 3.2.

2. Methods

We focus on convolutional neural networks (Zeng et al., 2016; Nguyen et al., 2016; Shadab et al., 2020; Trabelsi et al., 2019) and natural language processing (Le and Mikolov, 2014; Agarwal et al., 2019; Dutta et al., 2018).

Whenever available, we first compare the performance of the models on the same dataset used in the publication, and then, on alternative similar datasets. In addition, we modify the model characteristics incrementally and test the effect of the change on the model performance. More details on Section 2.2 for convolutional neural networks and on Section 2.3 for natural language processing.

| Dataset | Sample size | Sequence Length (bp) | Reference |
|-----------------|-------------|----------------------|----------------------|
| Histone | 14965 | 500 | Nguyen et al. (2016) |
| Splice | 3190 | 60 | Nguyen et al. (2016) |
| Promoter | 106 | 58 | Nguyen et al. (2016) |
| Motif discovery | 269100 | 101 | Zeng et al. (2016) |
| ChIP-seq toy | 97718 | 101 | Zeng et al. (2016) |

Table 1: Datasets used to test the neural network models.

2.1 Available Datasets

We focus on five datasets from the available ones in the papers under study (Table 1):

Histone data. Nguyen et al. (2016) included 10 datasets about DNA sequences wrapping around histone proteins. We will focus on the H3 occupancy from the histone dataset that has 14965 sequences of length 500 bp. The H3 indicates the histone type, and the dataset has two classes: the positive class are DNA sequences that contains regions wrapping around histone proteins and the negative class does not.

Splice data. Nguyen et al. (2016) included a splice dataset (also in the UCI machine learning repository (Dua and Graff, 2017)). Splice junctions are points on a DNA sequence at which superfluous DNA is removed during the process of protein creation in higher organisms. This dataset has 3190 sequences of length 60 bp and are classified into three classes: exon/intron boundaries (EI), intron/exon boundaries (IE), and non-splice (N).

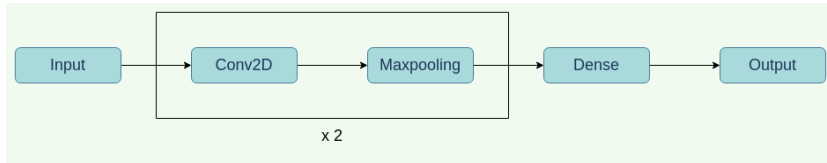
Promoter data. Nguyen et al. (2016) included a promoter dataset (also in the UCI machine learning repository (Dua and Graff, 2017)). A promoter is a sequence of DNA to bind proteins that initiate transcription from downstream DNA. This dataset has 106 sequences of length 57 bp and are classified into two classes: promoters and non-promoters.

Motif discovery data. Zeng et al. (2016) included two ChIP-seq datasets: motif discovery and motif occupancy. These datasets contain the labels of the binding affinity of transcription factors to DNA sequence in 690 different ChIP-seq experiments. We will only focus on a subset of 269100 sequences from the motif discovery data (out of 20464149) of length 101.

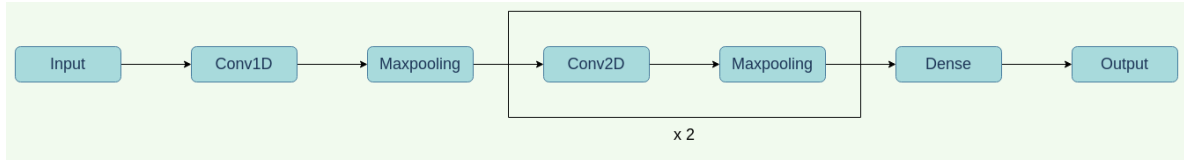
ChIP-seq toy data. This is a subset of the ChIP-seq data provided by Zeng et al. (2016) of 97718 sequences of length 101 bp. It is unclear if this subset was taken from the motif discovery data or the motif occupancy as the authors do not provide this information. However, given the sequence length, it appears that this subset comes from the motif discovery data.

2.2 Convolutional Neural Networks

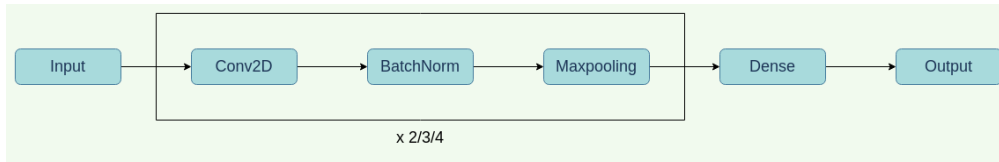
We test the performance of four convolutional neural network (CNN) models found in literature (Zeng et al., 2016; Nguyen et al., 2016; Shadab et al., 2020; Trabelsi et al., 2019) that have been successful on genomic-based prediction. We assess their performance on their own datasets (when available) and on alternative similar datasets, as well as under incremental modifications of the model characteristics such as data encoding, window size and number of layers. See Table 2 for a summary of the performance tests and models.



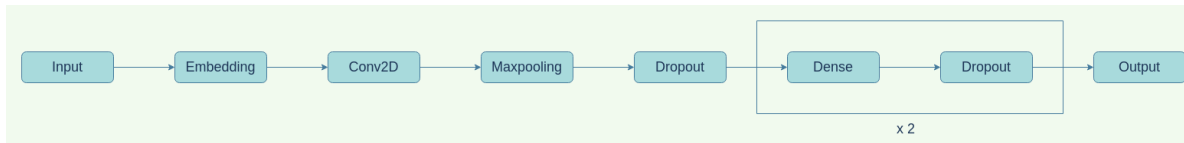
(a) Original CNN-Nguyen (Nguyen et al., 2016)



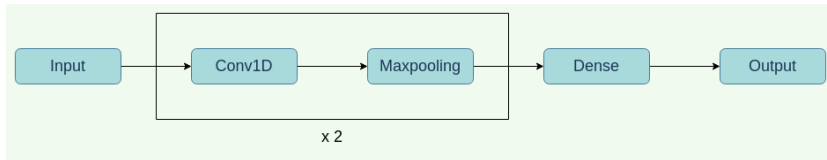
(b) Modified CNN-Nguyen (Nguyen et al., 2016)



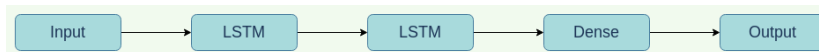
(c) Original CNN-Zeng (2 layers), modified (3,4 layers) (Zeng et al., 2016)



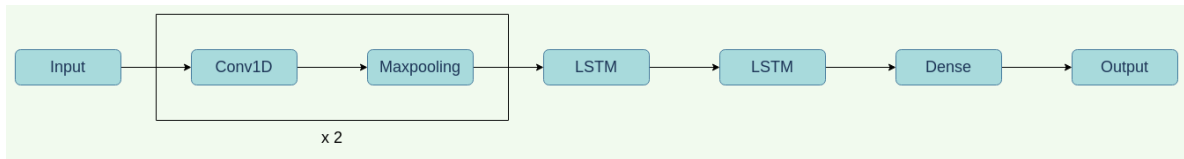
(d) DeepDBP (Shadab et al., 2020)



(e) DeepRAM-CNN (Trabelsi et al., 2019)



(f) DeepRAM-RNN (Trabelsi et al., 2019)



(g) DeepRAM-CNN-RNN (Trabelsi et al., 2019)

Figure 1: Convolutional Neural Network models

| | Model | Own datasets | Outside datasets | Performance tests |
|-------------------------------------|--------------------|---------------------------|------------------|--|
| CNN-Nguyen (Nguyen et al., 2016) | Figure 1a | histone, splice, promoter | motif discovery | number of layers, data robustness, dimension |
| CNN-Zeng (Zeng et al., 2016) | Figure 1c | motif discovery | | number of layers |
| DeepDBP (Shadab et al., 2020) | Figure 1d | | motif discovery | data robustness |
| DeepRAM (Trabelsi et al., 2019) | Figures 1e, 1f, 1g | | motif discovery | data encoding |

Table 2: CNN models along with the datasets used and the performance tests

2.2.1 CNN-NGUYEN (NGUYEN ET AL., 2016)

Datasets. We use the original datasets of the paper: histone, splice and promoter (Nguyen et al., 2016). The histone dataset is split into 70% for training, 15% for validation, and 15% for testing. The splice and promoter datasets are relatively small, so they are only split into 75% for training and 25% for testing.

Data encoding. As in Nguyen et al. (2016), we use a sliding window of fixed size across the sequence. At each step, a kmer is read from the window and added to the kmer sequence. For example, if a sequence looks like “ACTGG”, then its 3-mers are [“ACT”, “CTG”, “TGG”]. The process is similar to how ngrams are created from text. After that, one-hot encoding is applied to the kmers. To also include to spatial information of the sequences, we concatenate the encoding of k-mers within a fixed region size. As in Nguyen et al. (2016), we choose a window size of 3 and a region of 2.

Neural network model. We implement the simple neural network in Nguyen et al. (2016) as our baseline model (Figure 1a). The model contains two 2D convolutional layers, each followed by a pooling layer, then the output of the convolutional layers are connected to a fully connected layers. The fully connected layer has a dropout rate of 0.5 to reduce the effect of overfitting. Finally, we use a softmax layer to predict the labels of the input sequences.

Performance tests. We perform three tests with this model: 1) we replicate the results in (Nguyen et al., 2016), 2) we compare the performance of the model with a different dimension (1D) and increasing number of layers (Figure 1b), and 3) we test the robustness of the model (with and without transfer learning) when fitted to the alternative motif discovery dataset (Zeng et al., 2016).

2.2.2 CNN-ZENG (ZENG ET AL., 2016)

Datasets. We used a subset of the original dataset: motif discovery data (Zeng et al., 2016). The subset is further split into 48.7% for training, 2.6% for validation, and 48.7% for testing.

Data encoding. We use the same encoding method as in the CNN-Nguyen model. The sequences are converted into kmers, one-hot encoded, and then concatenated with neighbouring kmers. Again, for consistency, we choose a window size of 3 and a region of 2.

Neural network model. We implement the neural network model in Zeng et al. (2016) (Figure 1c) that contains two 2D convolutional layers with unknown hyperparameters, so we also use a model that contains two 2D convolutional layers, each followed by a batch-normalization and max-pooling layer. The output of the convolutional layers is connected to a fully connected layer. This layer has a dropout rate of 0.5 to prevent overfitting. Finally, a softmax layer is used to predict the class of the input sequence.

Performance tests. To explore the effect of the number of layers, we add 2D convolutional, batch-normalization, and max-pooling layers to the end of the convolutional network (Figure 1c). The number of filters in convolutional layer doubles each time we add a new set of these layers (e.g. 16 filters in the first convolutional layer, 32 in the second, 64 in the third).

2.2.3 DEEPDBP (SHADAB ET AL., 2020)

Dataset. This paper did not provide any datasets, so we use the motif discovery dataset (Zeng et al., 2016).

Data encoding. To give fair comparison between all CNN models we tested, we use the same encoding method applied to the motif discovery dataset. The sequences are converted into kmers, one-hot encoded, and then concatenated with neighbouring kmers. Again, for consistency, we choose a window size of 3 and a region of 2.

Neural network model. The source code of this paper is not well structured and contains many different models that are not properly documented, so we are unable to identify the architecture of the DeepDBP model. However, we implemented a model based on the paper description that contains an embedding layer, a convolutional layer, max-pooling layer, followed by fully connected layers and the output layer (Figure 1d).

Performance tests. We test the robustness of the proposed architecture to the motif discovery dataset (Zeng et al., 2016) and see if the achieved prediction accuracy is comparable to the one reported in the paper.

2.2.4 DEEPRAM (TRABELSI ET AL., 2019)

Dataset. This paper did not provide any datasets, so we use the motif discovery dataset (Zeng et al., 2016).

Data encoding. We experiment with two different ways of encoding the sequences. One way is, as described before, to use one-hot encoding with word size 3 and region size 2. The other way is to convert sequences into overlapping kmers, and embed kmers into dense vectors using embedding layers. Note that this embedding is different from the one used in Section 2.3 because of the unit used for encoding. Here, we use the kmer as the unit for encoding while in LSTM-AE, we use the nucleotide as the unit.

Neural network model. We implement the three models in Trabelsi et al. (2019): 1D convolutional neural networks (Figure 1e), recurrent neural networks (Figure 1f), and a mixture of 1D convolutional and recurrent neural networks (Figure 1g). For convolutional neural networks, we use two 1D convolutional layers, with each followed by a max-pooling layer, and finally fully connected layers and output layer. For recurrent neural networks, we use two Long Short-Term Memory (LSTM) layers followed by fully connected layers and output layer. For the hybrid neural networks, we use two 1D convolutional layers and two Long short-term memory layers, and finally fully connected layers and output layers. We

| | Model | Own datasets | Outside datasets | Performance tests |
|--------------------------------------|----------------------|--------------|--------------------|---------------------|
| LSTM-layer | Figure 2a | | ChIP-seq splice | toy, optimizer |
| doc2vec+NN (Le and Mikolov, 2014) | Figure 2d | | ChIP-seq splice | toy, embedding size |
| LSTM-AE+NN (Agarwal et al., 2019) | Figures 2b and 2d | | ChIP-seq splice | toy, batch size |

Table 3: NLP models along with the datasets used and the performance tests

note that the DeepRAM-RNN and the DeepRAM-CNN-RNN models are not entirely CNN models and share many characteristics with the models presented in Section 2.3. However, we present these models in this section given that they are all part of the DeepRAM paper (Trabelsi et al., 2019) and we follow the comparisons and analyses highlighted in this work. *Performance tests.* We compare the changes in performance based on the data encoding.

2.3 Natural Language Processing Neural Networks

Traditionally, genomic data is stored as a collection of long strings comprised of the four nucleotides: A,C,G,T. It is thus intuitive to turn to Natural Language Processing (NLP) theory for solid ways to embed the sequences in a latent space. Furthermore, NLP methods naturally overcome one of the main drawbacks of CNN models which is the sparsity of the input vectors.

Here, we focus on two widely used NLP tools: doc2vec (Le and Mikolov, 2014) and Long Short Term Memory (LSTM) (Agarwal et al., 2019; Kimothi et al., 2016). Both methods share the same objective: represent the input sequence with a low dimensional dense vector yet the specifics differ as is explained below.

We first clarify that the NLP methods are not performing prediction (as the CNN models were in Section 2.2). Since the purpose of this work is to compare the performance of neural network models on the prediction of phenotypes from genomes, we need to add a neural network model to the NLP model that will perform the prediction of labels (Figure 2d).

Table 3 presents a summary of the performance tests and models. In addition to those tests, we compare the prediction accuracy of the three models and we compare the auto-encoding potential of doc2vec and LSTM-AE.

2.3.1 LSTM-LAYER

Datasets. We use the ChIP-seq toy dataset which is a subset of the motif discovery data from Zeng et al. (2016) which had already been separated into training/validation/test sets (77174/1000/19544 sequences respectively). The length of each sequence is 101. As described in the motif discovery data, the sequences have binary classes and the class distribution in each set is fairly even. In addition, we use the splice data in Nguyen et al. (2016) which we split into training set, validation set, and test set with 2041, 511, and 638 samples respectively.

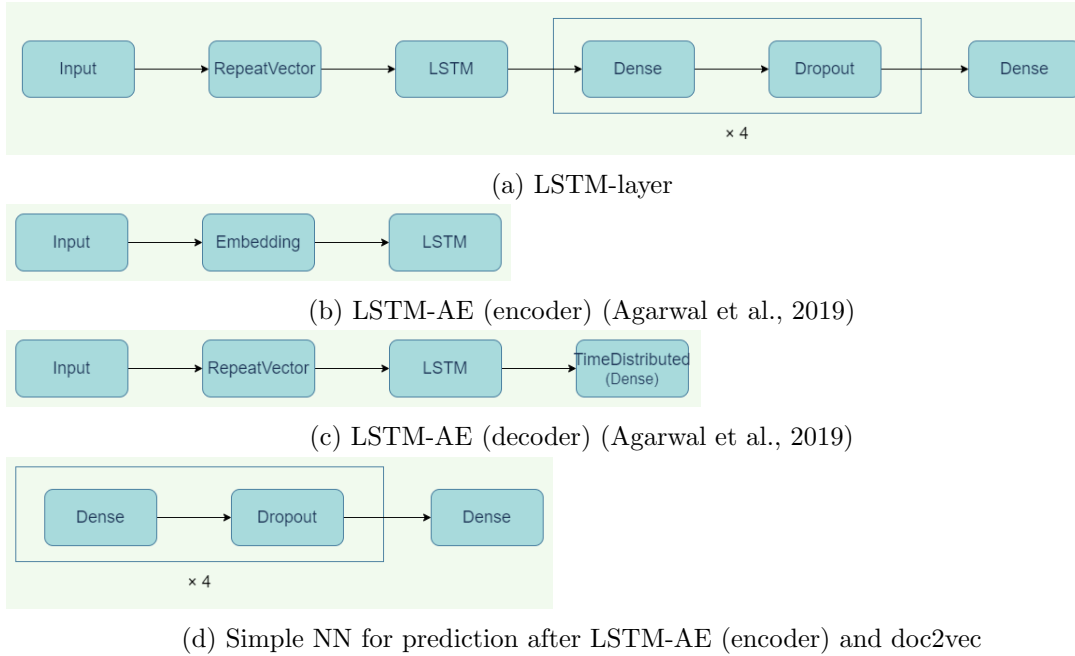


Figure 2: Natural Language Processing Neural Network models

Data encoding. Each nucleotide is converted to a label number. For example, [“A”, “C”, “G”, “T”], are encoded as [3, 2, 1, 0] in descending lexicographical order. The LSTM-layer is crucial given the intractable growth in dimension of the input vector. That is, a sequence containing 6000 nucleotides would be represented by a sequence of 6000 numbers.

Neural network model. We implement the neural network model (Figure 2a) that contains, after the input layer, an embedding layer followed by an LSTM layer with size of 30 for both datasets. There are four dense layers with size decaying by a factor of 2 (128-64-32-16). There is one Dropout layer between any two Dense layers with dropout rate of 0.2.

Performance tests. We compare the prediction accuracy of this model with the other two NLP models: doc2vec+NN and LSTM-AE+NN. In addition, we study the changes in performance when using different optimizers.

2.3.2 DOC2VEC+NN (LE AND MIKOLOV, 2014)

Datasets. We use the same two datasets already described in LSTM-layer: ChIP-seq toy (Zeng et al., 2016) and splice (Nguyen et al., 2016).

Data encoding. We encode the sequences based on 3-mers with window size of 1. For example, for the “ACTGG” sequence, the 3-mers are [“ACT”, “CTG”, “TGG”]. We construct a dictionary with all the 3-mers in the training set. While it is unlikely for 3-mers in the test set to not appear in the dictionary, we categorize these instances as out-of-vocabulary (OOV) with a unique encoding.

Neural network model. The nature of the doc2vec sequence representation as a semantic vector preserves similarity of sequences in terms of frequency and location of ngrams. We apply the distributed memory mode (DV-PM) as in Le and Mikolov (2014), and then, we

use the simple fully connected neural network in Figure 2d containing two dense layer with size shrinking by a factor of 2 with a dropout layer in between.

Performance tests. We compare the prediction accuracy of this model with the other two NLP models: LSTM-layer and LSTM-AE+NN. In addition, we study the effect of embedding size in the performance of the model. Finally, we compare the encoding potential (ability to recover the original sequences) of doc2vec and LSTM-AE.

2.3.3 LSTM-AE+NN (AGARWAL ET AL., 2019)

Datasets. We use the same two datasets already described in LSTM-layer: ChIP-seq toy (Zeng et al., 2016) and splice (Nguyen et al., 2016).

Data encoding. We use the same encoding as in the LSTM-layer model. Each nucleotide is converted to a label number. For example, ["A", "C", "G", "T"], are encoded as [3, 2, 1, 0] in descending lexicographical order.

Neural network model. A LSTM autoencoder model (LSTM-AE) aims to represent a sequence by a dense vector that can be converted back to the original sequence. Indeed, LSTM-AE is comprised of two parts: an encoder network (Figure 2b) that compresses the original sequence into a low dimensional dense vector, and a decoder network (Figure 2c) that converts the vector back to the original sequence. The encoder reads as input an encoded DNA sequence and outputs a dense vector as the embedding for this sequence whose length is a hyper parameter to tune. The decoder reads as input the dense vector produced by the encoder and produces a reconstructed sequence. The accuracy of the autoencoder is measured by comparing the reconstructed sequence to the original sequence.

We implement a LSTM-AE following Agarwal et al. (2019) based on the description in their publication given that no reproducible script was available. The LSTM-AE model is trained to achieve maximum reconstruction accuracy of the sequences. Then, since LSTM-AE is not performing classification, we add a simple fully connected neural network (Figure 2d) containing two dense layer with size shrinking by a factor of 2 with a dropout layer in between for the prediction of class labels. The size of the first dense layer is adjusted, as a rule of thumb, to match 1 to 4 times the embedding dimension. We denote this model as LSTM-AE+NN. We note that only the weights corresponding to the simple fully connected neural network are optimized for classification which is different to the LSTM-layer model whose embedding indeed changes during training. We highlight that the LSTM-layer and LSTM-AE models differ on how an embedding is evaluated. The embedding produced by the LSTM-layer model aims to better classify the sequences into the right category while the embedding produced by the LSTM-AE model aims to better capture the sequence itself.

Performance tests. We compare the prediction accuracy of this model with the other two NLP models: LSTM-layer and doc2vec+NN. In addition, we study the effect of the batch size in the performance of the model. Finally, we compare the encoding potential (ability to recover the original sequences) of LSTM-AE and doc2vec.

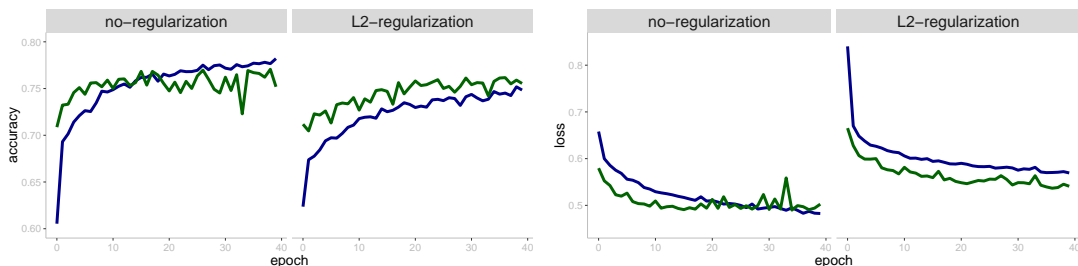


Figure 3: Learning dynamics for the original CNN-Nguyen model with two 2D convolutional layers (Figure 1a) on the histone data. Color represents training (blue) or validating (green) accuracy or loss. Even without regularization, there is not any evidence of overfitting. With L2 regularization, the validation accuracy does not change much, but the overall loss increases.

3. Results

3.1 Convolutional Neural Networks

3.1.1 REPLICATION OF RESULTS

First, DeepDBP (Shadab et al., 2020) did not provide data or reproducible scripts of the analyses, and thus, we were unable to replicate the results. DeepRAM (Trabelsi et al., 2019) does provide open-source software (<https://github.com/MedChaabane/deepRAM>), but they did not provide details or public links on the datasets used. Thus, we decided to use existing data (Table 1) to test the models in both DeepDBP and DeepRAM.

The CNN-Nguyen model (Nguyen et al., 2016) shows good performance on the histone data (78.2% training accuracy, 77.1% validation accuracy in Figure 3) and there is little evidence of overfitting. The accuracy that we obtain is slightly different to the one reported in the paper. Despite the lack of evidence of overfitting, we add an L2 regularization which increases the loss and decreases the accuracy (75.2% training accuracy, 76.2% validation accuracy in Figure 3).

For splice and promoter datasets, an even simpler neural network model (only one 2D convolutional layer) performs quite well (100% and 100% validation accuracy respectively, figure in the Supplementary Material). The original paper used a model with two 2D convolutional layers, and has got an accuracy of 96.1% and 99.1% for splice and promoter dataset respectively.

For the CNN-Zeng model (Zeng et al., 2016), we observe clear underfitting to their own motif discovery data (64.8% training accuracy, 64.1% validation accuracy, Figure 5 first column). These results do not match the results in the original paper, yet we are considering a subset of the original data which could be the source of the difference in performance.

3.1.2 THE ROLE OF CONVOLUTIONAL LAYERS AND DIMENSION.

We add one additional convolutional 1D layer to CNN-Nguyen (Nguyen et al., 2016), and compare the performance with the original model. The rationale for the added layer is that

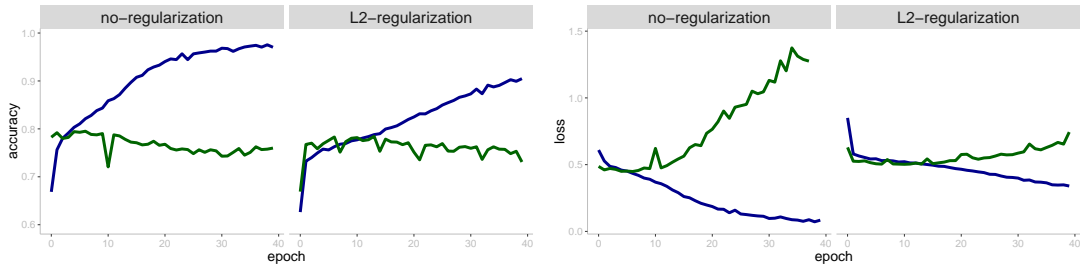


Figure 4: Learning dynamics for modified CNN-Nguyen with one extra 1D convolutional layer (Figure 1b) on the histone data. Color represents training (blue) or validating (green) accuracy or loss. There is evidence of overfitting without regularization which is somewhat alleviated by an L2 regularization.

the sequences in the histone data are relatively long (500 bp), so in order to shorten the input, we add a 1D convolutional layer before the 2D convolutional layers to shorten the input into equal width and height (e.g. $192 \times 192 \times n_{filters}$). We find that this model suffers from severe overfitting (97.5% training accuracy, 79.5% validation accuracy in Figure 4). Adding an L2 regularization reduces the effect of overfitting (90.5% training accuracy, 78.4% validation accuracy in Figure 4), but does not improve validation accuracy significantly.

Regarding the dimension, we compare the performance of the one 2D convolutional model of CNN-Nguyen on the splice and promoters datasets (already quite accurate with 93.9% and 100% validation accuracy, see Section 3.1.1) to a model with one 1D convolutional layer instead. We find that the performance is comparable (96.1% and 100% validation accuracy respectively, figure in the Supplementary Material) which gives us evidence that in this case, the dimension is not playing an important role in prediction.

With the CNN-Zeng model Zeng et al. (2016), we test if more 2D layers improve the prediction accuracy given that the original model with two convolutional layers suffers from underfitting in their own motif discovery data (64.8% training accuracy, 64.1% validation accuracy). When adding a new layer (total of three convolutional layers), the accuracy is improved (73.7% training accuracy, 69.7% validation accuracy in Figure 5).

The problem of overfitting emerges when we use four convolutional layers (80.1% training accuracy, 68.2% validation accuracy in Figure 5). Therefore, we apply L2 regularization on the CNN-Zeng model with four layers which indeed reduces the effect of overfitting (69.0% training accuracy, 69.6% validation accuracy in Figure 6), but it also limits the learning power of the model by yielding a lower prediction accuracy overall. It appears that having 3 convolutional layers was the sweet spot between underfitting and overfitting for this particular dataset.

3.1.3 ROBUSTNESS ACROSS DATASETS

We test if the model in CNN-Nguyen (Nguyen et al., 2016) and the DeepDBP model (Shadab et al., 2020) could work successfully on the motif discovery data from Zeng et al. (2016).

When we train the CNN-Nguyen model Nguyen et al. (2016) on the motif discovery data (Zeng et al., 2016), the validation accuracy is not great (59.3%), so we try transfer learning by first training the model on the splice dataset (validation accuracy 93.9%) and

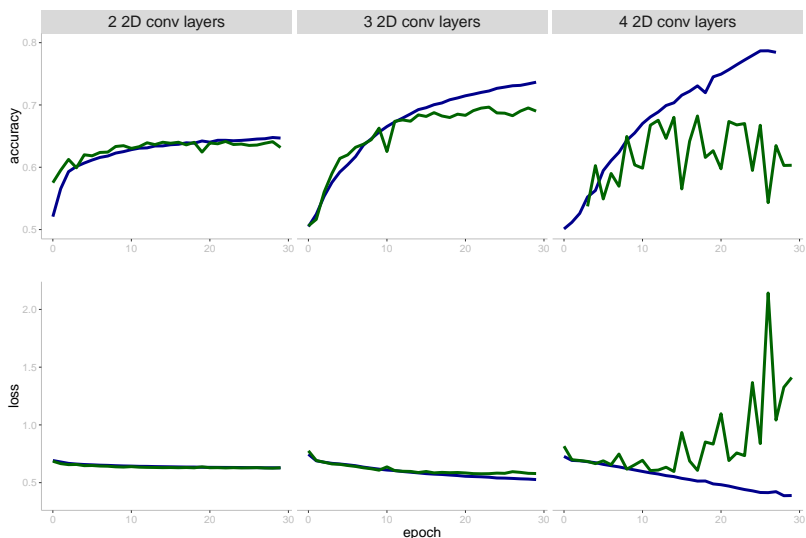


Figure 5: Learning dynamics for the CNN-Zeng models with two (the original), three, or four 2D convolutional layers (Figure 1c) in the motif discovery data. Color represents training (blue) or validating (green) accuracy or loss. The model with only 2 layers (left) exhibits underfitting. The model with 3 layers (middle) exhibits a certain degree of overfitting which can be argued as acceptable. The model with 4 layers (right) exhibits clear overfitting. The pattern is consistent with the knowledge that more complex models tend to overfit.

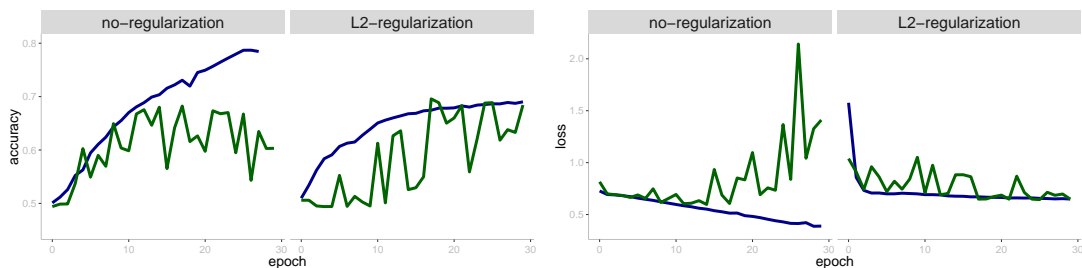


Figure 6: Learning dynamics for the CNN-Zeng model with four 2D convolutional layers (Figure 1c) in the motif discovery data. Color represents training (blue) or validating (green) accuracy or loss. The model suffers from overfitting which is improved via L2 regularization.

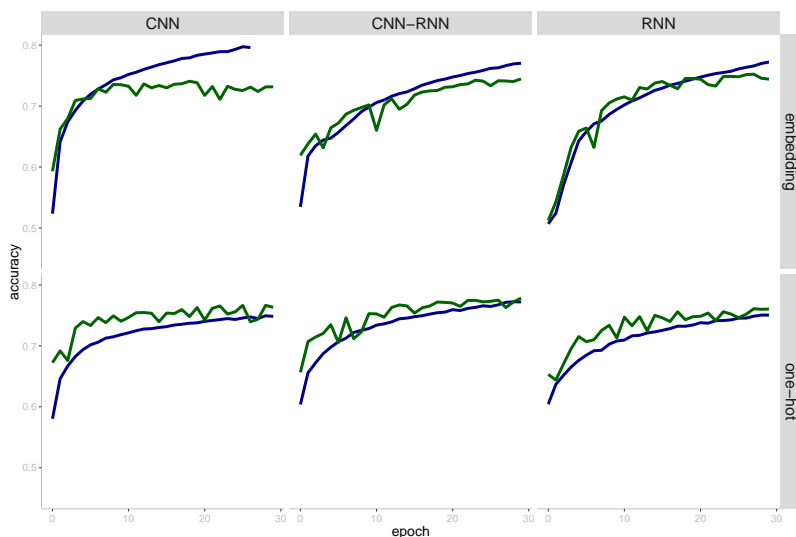


Figure 7: Learning dynamics for the DeepRAM models (Figures 1e, 1f, 1g) on the motif discovery data. Rows correspond to different data encodings (embedding and one-hot encoding). Columns correspond to different architectures (convolutional neural networks, convolutional plus recurrent neural networks, and recurrent neural networks). Color represents training (blue) or validating (green) accuracy. Plots for loss function are in the Supplementary Material.

then training the pre-trained model on the motif discovery data. The validation accuracy is improved, but not dramatically (60.3%). We conclude that the model is not robust across datasets even with transfer learning. One possible explanation for the lack of improvement with transfer learning is that the pre-trained model is only trained on a very small dataset (3190), and the new dataset is fairly large (269100), so the model did not learn anything that is transferable.

Finally, we find that the DeepDBP model (Shadab et al., 2020) does not perform very well on the motif discovery dataset (Zeng et al., 2016). The accuracy does not change very significantly during the training time, fluctuating around 50%.

3.1.4 THE ROLE OF DATA ENCODING

We use the architectures of DeepRAM in Trabelsi et al. (2019) to test performance changes due to data encoding.

We find that all the combinations of the two encoding methods and three types of models give reasonable performance (around 75% validation accuracy) and rarely suffer from overfitting (Figure 7). In particular, the combination of using one-hot encoding and 1D convolutional and recurrent neural network gives the highest validation accuracy (77.8%). As a point of comparison, the accuracy presented in original DeepRAM paper ranges from 83.6% to 99.4%

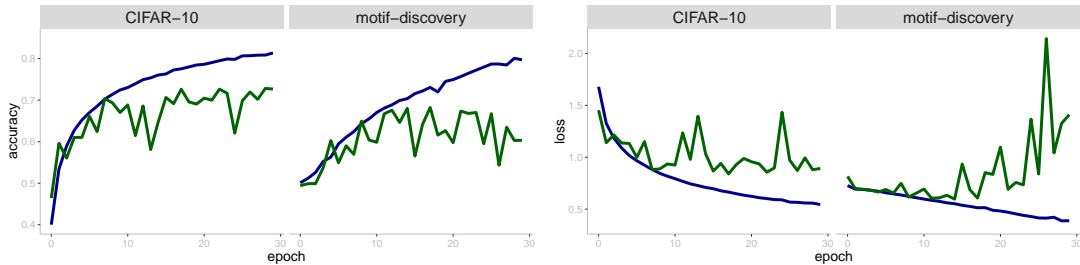


Figure 8: Learning dynamics for the four 2D convolutional layered model trained on the CIFAR-10 data and motif discovery data. Color represents training (blue) or validating (green) accuracy or loss. We perceive overfitting on both data.

| Model | Dataset | Training | Validation | Testing |
|------------|--------------|----------|------------|---------|
| LSTM-layer | ChIP-seq toy | 92.64% | 91.20% | 90.62% |
| LSTM-AE+NN | ChIP-seq toy | 67.60% | 67.50% | 66.50% |
| LSTM-layer | splice | 90.98% | 85.52% | 87.77% |
| LSTM-AE+NN | splice | 91.50% | 89.80% | 91.10% |

Table 4: Classification accuracy for the NLP models. The classification accuracy of doc2vec+NN was always close to 50% for both datasets.

3.1.5 THE ROLE OF SPARSITY IN OVERFITTING

We wonder if the overfitting on CNN-Zeng (4 CNN layers) is related to sparsity of genomic data. We train a model with four convolutional and pooling layers on both the motif discovery dataset and the CIFAR-10 dataset (Krizhevsky et al.). We observe that loss curves show similar overfitting pattern (Figure 8), so it appears that the overfitting is not related to the sparsity of the one-hot encoded sequence data.

3.2 Natural Language Processing Neural Networks

3.2.1 COMPARISON OF CLASSIFICATION ACCURACY

Table 4 shows the classification accuracy of LSTM-layer (Figure 2a) and LSTM-AE+NN (Figures 2b and 2d) models on the two datasets. LSTM-layer outperforms LSTM-AE+NN in the ChIP-seq data, while LSTM-AE+NN outperforms LSTM-layer on the splice data. The performance of doc2vec+NN is not shown since the classification accuracy was never far above 50% for these datasets. Figures for the learning dynamics of all models can be found in the Supplementary Material.

One conjecture for the poor performance of doc2vec is the short length of the sequences (60 in the splice data and 101 in the ChIP-seq data). We therefore decide to test the performance of doc2vec on a dataset of 281 sequences of length 4132 classified as *Potyvirus* and *Picornavirus*. This dataset belongs to our collaborators and is soon to be published, but it remains unpublished at the time of submission of this work (see Acknowledgements).

The doc2vec+NN model performs well on longer sequences with training prediction accuracy of 97.32% and testing prediction accuracy of 96.49%. The LSTM-layer model,

| Model | Subset | Length | Missingness | Training | Testing |
|------------|----------|--------|-------------|----------|---------|
| doc2vec+NN | complete | 4132 | 90.58% | 97.32% | 96.49% |
| LSTM-layer | complete | 4132 | 90.58% | 56.42% | 56.14% |
| LSTM-layer | MDL | 2449 | 84.82% | 62.01% | 59.65% |
| LSTM-layer | front | 2449 | 91.50% | 93.85% | 96.49% |
| LSTM-layer | rear | 2449 | 88.48% | 54.19% | 54.39% |

Table 5: Classification accuracy of different truncated versions of the virus dataset on doc2vec+NN and LSTM-layer models. The doc2vec+NN model outperforms LSTM-layer on every case, but it is evident that the performance of LSTM-layer does not depend exclusively on the length of the sequences.

however, performs worse on longer sequences with training prediction accuracy of 56.42%/ and testing prediction accuracy of 56.14% (LSTM-AE+NN has similar poor performance, results not shown).

To investigate the reasons for the poor performance of LSTM-layer (and LSTM-AE+NN) on the longer sequences, we reduce the sequence length on the virus dataset to 2449 bp based on three criteria: 1) using a phylogenetic-based approach denoted MDL (Ané, 2011), 2) keeping the first 2449 nucleotides in the sequence and 3) keeping the last 2449 nucleotides in the sequence. The number 2449 was determined by MDL.

Table 5 shows that doc2vec+NN outperforms LSTM-layer on all cases of reduced sequence length, yet the performance of LSTM-layer does not appear to depend exclusively on the sequence length. Indeed, LSTM-layer has its best performance when keeping the first 2449 nucleotides of the sequence. This pattern is not explained either by the percentage of missing nucleotides (labeled “N”) in the sequences. Biologically, DNA sequences contain important information about translation at the beginning of the sequence which could in part explain why the performance is improved when keeping this region. We conclude that doc2vec+NN seems to provide a better embedding for the accurate classification for long sequences compared to LSTM-layer (or LSTM-AE+NN).

3.2.2 THE ROLE OF THE EMBEDDING SIZE ON CLASSIFICATION ACCURACY OF DOC2VEC+NN

We compare the performance of the doc2vec+NN classification accuracy on the virus dataset on different embedding sizes (Table 6 and Figure in the Supplementary Material). Embedding size of 100 produces the best performance of all, but results do not differ much among the sizes selected for the experiment.

3.2.3 THE ROLE OF THE OPTIMIZER IN THE CLASSIFICATION ACCURACY OF THE LSTM-LAYER MODEL

Table 7 and Figure 9 show that the Stochastic Gradient Descent (SGD) optimizer outperforms the Adam optimizer in the training of the LSTM-layer model (Figure 2a) for the splice data (and in the Supplementary Material for the ChIP-seq toy data). Reddi et al. (2019) have already discussed the convergence issues of the Adam optimizer. We had to be careful, however, when using Early Stop Callback with the SGD optimizer as training

| Embedding size | Training | Testing |
|----------------|----------|---------|
| 50 | 90.63% | 87.72% |
| 100 | 97.32% | 96.49% |
| 150 | 95.98% | 94.74% |
| 200 | 94.20% | 92.98% |

Table 6: Classification accuracy of doc2vec+NN model on the virus dataset for different embedding sizes. Embedding size of 100 produces the best performance.

| Dataset | Optimizer | Training | Validation | Testing |
|--------------|-----------|----------|------------|---------|
| ChIP-seq toy | Adam | 92.64% | 91.20% | 90.62% |
| ChIP-seq toy | SGD | 94.08% | 90.40% | 91.70% |
| splice | Adam | 86.82% | 78.28% | 80.25% |
| splice | SGD | 90.98% | 85.82% | 87.77% |

Table 7: Classification accuracy of the LSTM-layer model on different optimizers and different datasets. SGD seems to outperform Adam on the cases compared.

would stop much earlier than desirable and thus, Adam would outperform SGD. While we used Early Stop Callback on both Adam and SGD optimizers, the patience parameter was quite different. The patience parameter is a threshold to stop the training if the loss stops decreasing further after a certain number of epochs. We set the patience at 100 for Adam and at 400 for SGD which moves slower compared to Adam.

3.2.4 THE ROLE OF THE BATCH SIZE IN THE CLASSIFICATION ACCURACY OF THE LSTM-AE+NN MODEL

While training the LSTM-AE model (Agarwal et al., 2019) on the ChIP-seq toy data, we notice a strange pattern of sudden huge increments in loss (or decrements in accuracy). The pattern appears to be related to the batch size and learning rate. Increasing the batch size has very similar effects as decreasing the learning rate. A larger batch size enables the optimizer to better estimate the gradient for each step.

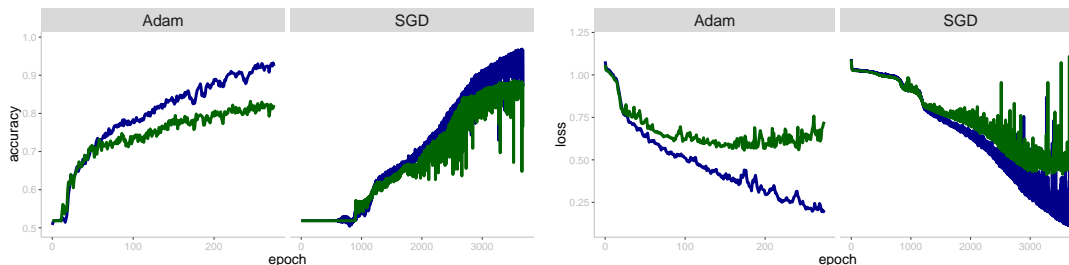


Figure 9: Learning dynamics for LSTM-layer model trained on the splice data with two optimizers: Adam and SGD. Color represents training (blue) or validating (green) accuracy or loss. Note that there are different number of epochs on each optimizer due to the speed of convergence.

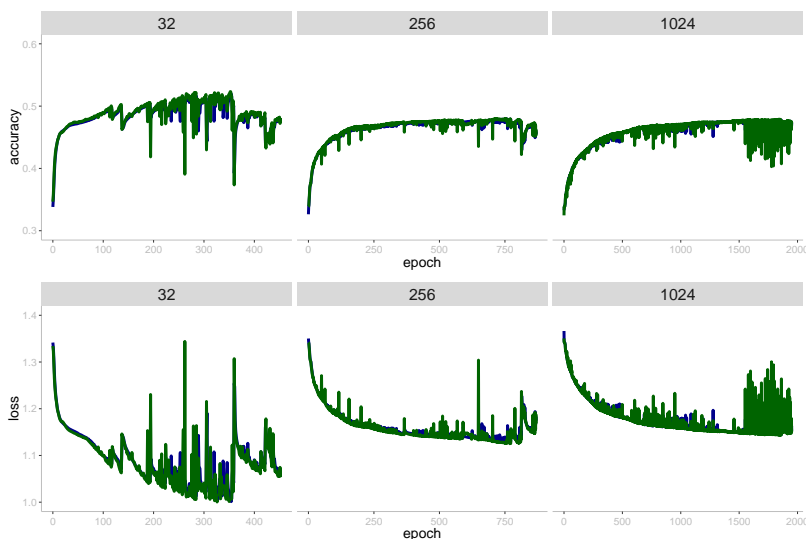


Figure 10: Learning dynamics of the LSTM-AE+NN classification model on the ChIP-seq toy data by different batch sizes (columns): 32, 256 and 1024. Color represents training (blue) or validating (green) accuracy or loss.

| Batch size | Training time per epoch | Training | Validating | Testing |
|------------|-------------------------|----------|------------|---------|
| 32 | 38s | 58.50% | 57.70% | 57.30% |
| 256 | 15s | 66.10% | 67.60% | 65.40% |
| 1024 | 13s | 67.60% | 67.50% | 66.50% |

Table 8: Classification accuracy per batch size for the LSTM-AE+NN model on the ChIP-seq toy data. Training time corresponds to the encoder network.

We compare different batch sizes in Table 8 and in Figure 10. We use the Adam optimizer with learning rate of 0.001.

Figure 10 shows that the sudden increments in loss (corresponding to sudden drops in accuracy) can be largely explained by the randomness of small batches as increasing the batch size alleviates this behavior with batch size of 256 showing the best performance. Interestingly, the effectiveness of the embedding is not affected by the erratic behavior of the learning dynamic (Table 8). Larger batch sizes have the added benefit of reducing the training time per epoch in the encoder network.

3.2.5 COMPARISON OF SEQUENCE EMBEDDING IN DOC2VEC AND LSTM-AE

We compare the embedding potential of doc2vec and LSTM-AE without the prediction part of the model. That is, we explore the strengths and weaknesses of each embedding strategy. Given that doc2vec and LSTM-AE correspond to quite different embedding processes, we cannot compare them directly, but we investigate reconstruction accuracy for LSTM-AE and Silhouette score (Rousseeuw, 1987; Pedregosa et al., 2011) for doc2vec.

For the LSTM-AE model (Figures 2b and 2c), we compare the reconstruction accuracy for different batch sizes using the sparse categorical cross entropy metric with nucleotides

| Batch size | Training time per epoch | Training (reconstruction) | Testing (reconstruction) |
|------------|-------------------------|---------------------------|--------------------------|
| 32 | 38s | 48.12% | 48.10% |
| 256 | 15s | 45.96% | 46.24% |
| 1024 | 13s | 47.33% | 47.46% |

Table 9: Reconstruction accuracy of the LSTM-AE model for different batch sizes on the ChIP-seq toy data. The accuracy is not improved by batch size, but the training time per epoch is indeed reduced.

| Embedding size | Full dimension | | Low dimension | |
|----------------|----------------|------------|---------------|------------|
| | Training SS | Testing SS | Training SS | Testing SS |
| 50 | 0.22 | 0.11 | 0.29 | 0.12 |
| 100 | 0.37 | 0.23 | 0.41 | 0.23 |
| 150 | 0.05 | 0.03 | 0.26 | 0.04 |
| 200 | 0.13 | 0.07 | 0.22 | 0.01 |

Table 10: Silhouette Score (SS) on the doc2vec embedding of the virus dataset by embedding size. Full dimension corresponds to the score computed on the doc2vec embedding before any projection to a low dimensional space. Low dimension corresponds to the score after project to a low dimensional space via tSNE. The Silhouette Score is the highest for the embedding size of 100 which agrees our conclusion in Table 6.

coded as integers. As mentioned already, the accuracy is not affected by the batch size, but the training time is reduced dramatically.

For the doc2vec embedding, we cannot calculate any reconstruction accuracy since the model is not reconstructing the input sequences. We instead project the embedded sequences on a low dimensional space (tSNE) and assess whether there is a clear separation of classes. Intuitively, if the embedding is able to separate the classes in a low dimensional space, the embedding aids in the prediction task of the neural network model. We evaluate the separation of classes for different embedding sizes with the Silhouette Score (Rousseeuw, 1987; Pedregosa et al., 2011). A higher Silhouette Score corresponds to an embedding with better defined clusters. The Silhouette Score is defined as $(b - a) / \max(a, b)$ for a , the mean distance between a sample and all other points in the same class, and b , the mean distance between a sample and all other points in the next nearest cluster.

Table 10 shows the Silhouette Score by embedding sizes for doc2vec on the virus dataset.

Finally, we compute the Silhouette Score on the embedding produced by the LSTM-AE model on the virus dataset merely as a point of comparison. For the full dimensional embedding, the training score is 0.029 and the testing score is 0.063, while the training/testing scores for the tSNE projection of the embedding are 0.003/0.034. These scores are much smaller than those obtained with the doc2vec embedding which agrees with our conclusion that doc2vec is a better embedding strategy for long sequences.

4. Discussion

Neural network models provide endless opportunities for prediction and classification in biological applications (Peng et al., 2020; Alber et al., 2019), yet much remains unknown regarding the transferability of the performance across datasets. Robustness across datasets of similar nature is a key ingredient to translate neural network models into medical practice and into the agricultural or environmental field.

Here, we study the performance on genomic data of two widely used classes of neural network models: convolutional neural networks (CNN) and natural language processing (NLP). We find that simple CNN (few layers) are robust across different genomic datasets with moderately good performance that is transferable and generalizable. As expected, more convolutional layers cause overfitting which can be overcome by regularization in most cases. In the situations we study, more than 3 convolutional layers are not justified for the sake of robustness and for control of overfitting, and simpler models are preferable. Finally, we suspect that the overfitting pattern that we observe with increasingly complex CNN could be due to the inherent sparsity of genomic data. Yet we observe the same overfitting pattern when the input data are images providing evidence that it is not the data, but the model what causes the nature of overfitting.

Regarding embedding of the sequences, we identify two conclusions. First, we find that doc2vec embedding is more powerful with longer sequences while LSTM-AE is better for shorter sequences. Second, embedding within the neural network architecture (LSTM-layer) has better prediction accuracy than embedding first, and then predicting with a simple NN (doc2vec+NN and LSTM-AE+NN). However, when this embedding is done within a CNN (DeepRAM), it can lead to overfitting. Furthermore, the optimization problem of embedding layers can become intractable for large datasets.

We conclude by raising awareness to the importance of reproducibility in science. In many instances, it was impossible to replicate the results of existing publications given the lack of reproducible well-documented scripts and available data. Reproducibility is crucial not just for the sake of open science, but to maximize the applicability of our machine-learning findings into a biological or medical community who might not have a strong programming background.

4.1 Reproducibility

All the scripts are publicly available in the Github repository <https://github.com/solislemuslab/dna-nn-theory>.

Acknowledgments

This work is supported by the Department of Energy [DE-SC0021016 to CSL]. We thank Dr. Aurelie Rakotondrafara and Helena Jaramillo Mesa for the virus data which will be published soon as part of their own research. Finally, we acknowledge the work in Hotaling (2020) which helped us improve the scientific writing of this manuscript.

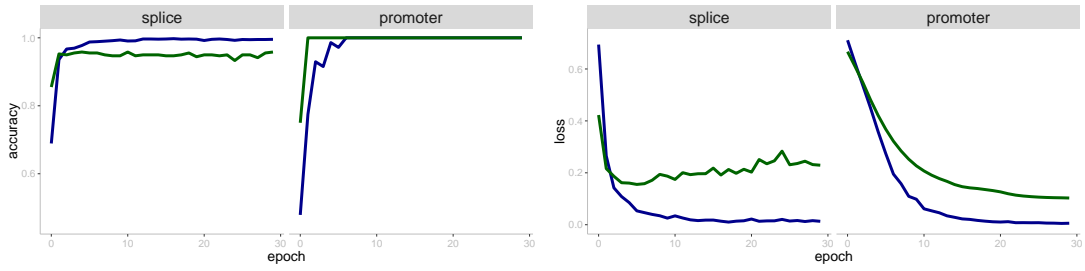


Figure 11: Learning dynamics for the simple CNN models that contain one 2D convolutional layer on splice and promoter data. Color represents training (blue) or validating (green) accuracy or loss.

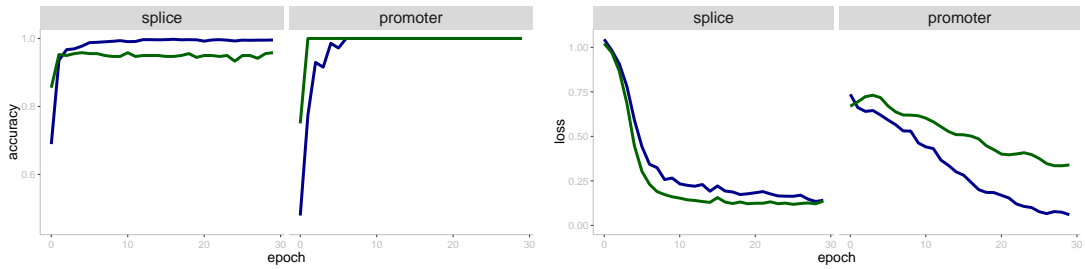


Figure 12: Learning dynamics for the simple CNN models that contain one 1D convolutional layer on splice and promoter data. Color represents training (blue) or validating (green) accuracy or loss.

Appendix A.

Reproducible Julia Script for Random Order of First Authors

```
using Random
s = 313627913
Random.seed!(s)
people = ["songyang","zhaoyi"]
people[randperm(length(people))]
```

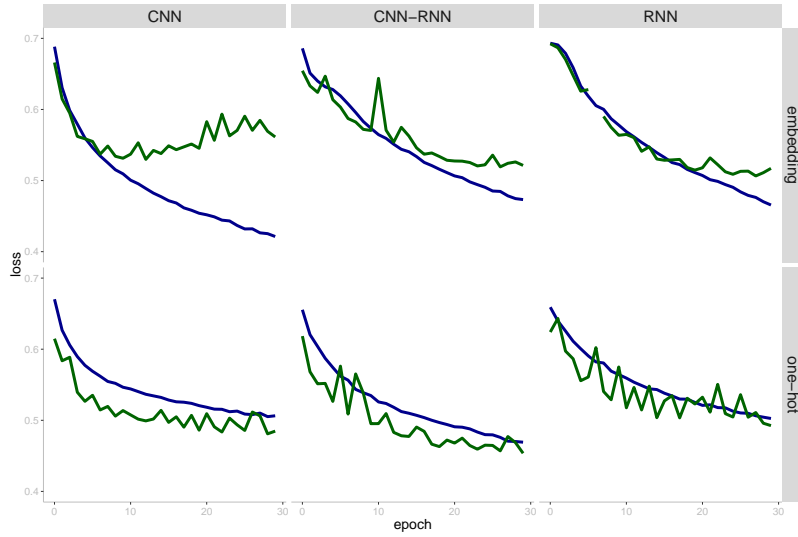


Figure 13: Learning dynamics for the DeepRAM models (Figures 1e, 1f, 1g) on the motif discovery data. Rows correspond to different data encodings (embedding and one-hot encoding). Columns correspond to different architectures (convolutional neural networks, convolutional plus recurrent neural networks, and recurrent neural networks). Color represents training (blue) or validating (green) loss.

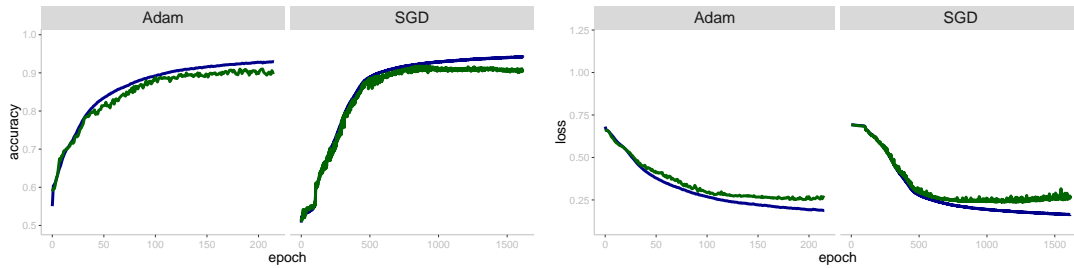


Figure 14: Learning dynamics on the LSTM-layer model on the ChIP-seq toy data by optimizer. Color represents training (blue) or validating (green) accuracy or loss.

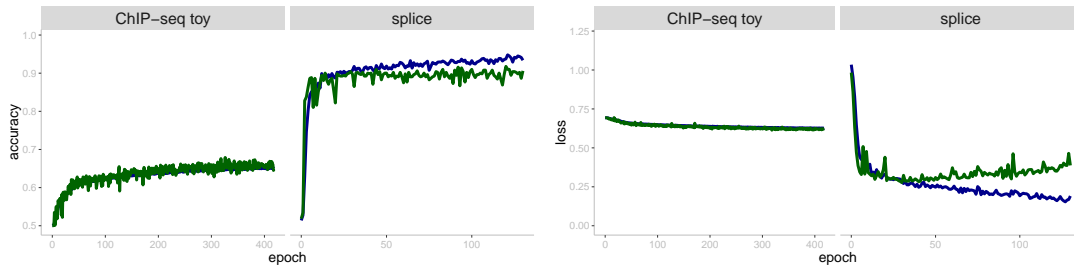


Figure 15: Learning dynamics of the LSTM-AE+NN classification model on ChIP-seq toy dataset and splice dataset. Color represents training (blue) or validating (green) accuracy or loss.

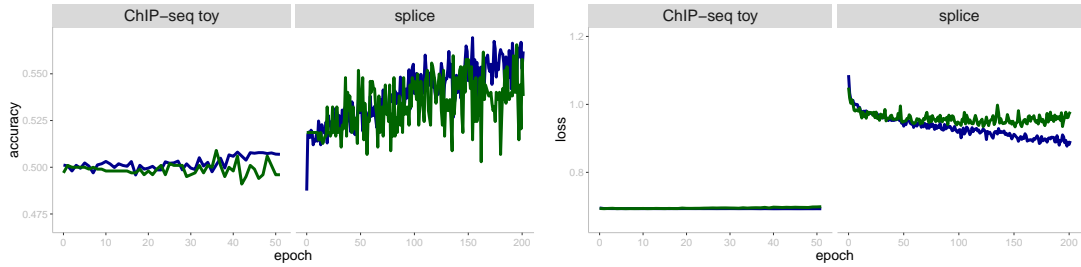


Figure 16: Learning dynamics of the doc2vec+NN classification model on ChIP-seq toy dataset and splice dataset. Color represents training (blue) or validating (green) accuracy or loss.

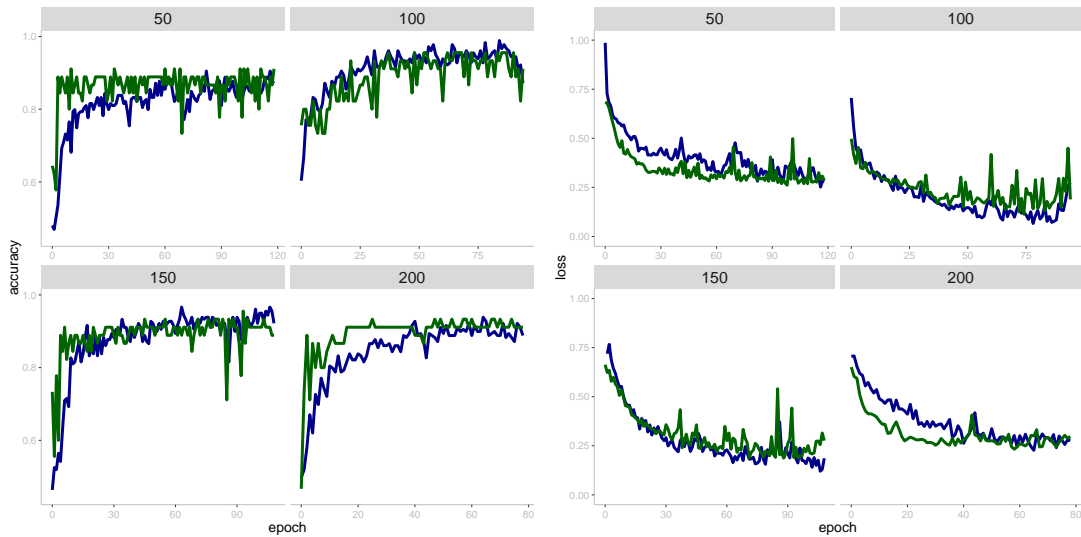


Figure 17: Learning dynamics of the doc2vec+NN classification model on the virus dataset depending on the embedding size: 50, 100, 150, and 200. Color represents training (blue) or validating (green) accuracy or loss.

References

- Vishal Agarwal, N Jayanth Kumar Reddy, and Ashish Anand. Unsupervised representation learning of DNA sequences. *arXiv*, (1906.03087), June 2019.
- Mark Alber, Adrian Buganza Tepole, William R Cannon, Suvranu De, Salvador Durabernal, Krishna Garikipati, George Karniadakis, William W Lytton, Paris Perdikaris, Linda Petzold, et al. Integrating machine learning and multiscale modeling—perspectives, challenges, and opportunities in the biological, biomedical, and behavioral sciences. *NPJ digital medicine*, 2(1):1–11, 2019.
- Cécile Ané. Detecting Phylogenetic Breakpoints and Discordance from Genome-Wide Alignments for Species Tree Reconstruction. *Genome Biology and Evolution*, 3:246–258, 02 2011. ISSN 1759-6653. doi: 10.1093/gbe/evr013. URL <https://doi.org/10.1093/gbe/evr013>.
- Euan A Ashley. The precision medicine initiative: a new national effort. *Jama*, 313(21): 2119–2120, 2015.
- Nicholas A Bokulich, Matthew R Dillon, Evan Bolyen, Benjamin D Kaehler, Gavin A Huttenhower, and J Gregory Caporaso. q2-sample-classifier: machine-learning tools for microbiome classification and regression. *Journal of open research software*, 3(30), 2018.
- Anna Paola Carrieri, Will PM Rowe, Martyn Winn, and Edward O Pyzer-Knapp. A fast machine learning workflow for rapid phenotype prediction from whole shotgun metagenomes. In *Proceedings of the AAAI Conference on Artificial Intelligence*, volume 33, pages 9434–9439, 2019.
- Hao-Xun Chang, James S Haudenschild, Charles R Bowen, and Glen L Hartman. Metagenome-wide association study and machine learning prediction of bulk soil microbiome and crop productivity. *Frontiers in Microbiology*, 8:519, 2017.
- Po-Hsuan Cameron Chen, Yun Liu, and Lily Peng. How to develop machine learning models for healthcare. *Nature Materials*, 18(5):410–414, 2019.
- Joana Rosado Coelho, João André Carriço, Daniel Knight, Jose-Luis Martínez, Ian Morrissey, Marco Rinaldo Oggioni, and Ana Teresa Freitas. The use of machine learning methodologies to analyse antibiotic and biocide susceptibility in staphylococcus aureus. *PLoS One*, 8(2):e55582, 2013.
- Maurizio Ferrari Dacrema, Paolo Cremonesi, and Dietmar Jannach. Are we really making much progress? a worrying analysis of recent neural recommendation approaches. In *Proceedings of the 13th ACM Conference on Recommender Systems*, RecSys ’19, page 101–109, New York, NY, USA, 2019. Association for Computing Machinery. ISBN 9781450362436. doi: 10.1145/3298689.3347058. URL <https://doi.org/10.1145/3298689.3347058>.
- Dheeru Dua and Casey Graff. UCI machine learning repository, 2017. URL <http://archive.ics.uci.edu/ml>.

- Julio M Duarte-Carvajalino, Diego F Alzate, Andrés A Ramirez, Juan D Santa-Sepulveda, Alexandra E Fajardo-Rojas, and Mauricio Soto-Suárez. Evaluating late blight severity in potato crops using unmanned aerial vehicles and machine learning algorithms. *Remote Sensing*, 10(10):1513, 2018.
- T. Dutta, A. and Dubey, K. K. Singh, and A. Anand. Splicevec: Distributed feature representations for splice junction prediction. *Computational biology and chemistry*, 74: 434–441, 2018.
- Michael Egmont-Petersen, Dick de Ridder, and Heinz Handels. Image processing with neural networks: a review. *Pattern recognition*, 35(10):2279–2301, 2002.
- Sean Ekins, Ana C. Puhl, Kimberley M. Zorn, Thomas R. Lane, Daniel P. Russo, Jennifer J. Klein, Anthony J. Hickey, and Alex M. Clark. Exploiting machine learning for end-to-end drug discovery and development. *Nature Materials*, 18(5):435–441, 2019.
- Christopher D Fjell, Håvard Jenssen, Kai Hilpert, Warren A Cheung, Nelly Pante, Robert EW Hancock, and Artem Cherkasov. Identification of novel antibacterial peptides by chemoinformatics and machine learning. *Journal of medicinal chemistry*, 52(7): 2006–2015, 2009.
- Erik Hjelmås and Boon Kee Low. Face detection: A survey. *Computer vision and image understanding*, 83(3):236–274, 2001.
- Daniel Sik Wai Ho, William Schierding, Melissa Wake, Richard Saffery, and Justin O’Sullivan. Machine learning snp based prediction for precision medicine. *Frontiers in Genetics*, 10:267, 2019.
- Scott Hotaling. Simple rules for concise scientific writing. *Limnology and Oceanography Letters*, 5(6):379–383, 2020. doi: <https://doi.org/10.1002/lol2.10165>. URL <https://aslopubs.onlinelibrary.wiley.com/doi/abs/10.1002/lol2.10165>.
- Ryan HL Ip, Li-Minn Ang, Kah Phooi Seng, JC Broster, and JE Pratley. Big data and machine learning for crop protection. *Computers and Electronics in Agriculture*, 151: 376–383, 2018.
- Eric Jonas, Monica Bobra, Vaishaal Shankar, J Todd Hoeksema, and Benjamin Recht. Flare prediction using photospheric and coronal image data. *Solar Physics*, 293(3):48, 2018.
- Gajendra Jung Katuwal and Robert Chen. Machine learning model interpretability for precision medicine. *arXiv preprint arXiv:1610.09045*, 2016.
- Erol S Kavvas, Edward Catoi, Nathan Mih, James T Yurkovich, Yara Seif, Nicholas Dillon, David Heckmann, Amitesh Anand, Laurence Yang, Victor Nizet, et al. Machine learning and structural analysis of mycobacterium tuberculosis pan-genome identifies genetic signatures of antibiotic resistance. *Nature communications*, 9(1):1–9, 2018.
- Dhananjay Kimothi, Akshay Soni, Pravesh Biyani, and James M. Hogan. Distributed representations for biological sequence analysis. *arXiv*, (1608.05949), 2016.

- Chayakrit Krittanawong, HongJu Zhang, Zhen Wang, Mehmet Aydar, and Takeshi Kitai. Artificial intelligence in precision cardiovascular medicine. *Journal of the American College of Cardiology*, 69(21):2657–2664, 2017.
- Alex Krizhevsky, Vinod Nair, and Geoffrey Hinton. Cifar-10 (canadian institute for advanced research). URL <http://www.cs.toronto.edu/~kriz/cifar.html>.
- Ahmet Kucuk, Juan M Banda, and Rafal A Angryk. A large-scale solar dynamics observatory image dataset for computer vision applications. *Scientific data*, 4:170096, 2017.
- Quoc Le and Tomas Mikolov. Distributed representations of sentences and documents. In Eric P. Xing and Tony Jebara, editors, *Proceedings of the 31st International Conference on Machine Learning*, volume 32 of *Proceedings of Machine Learning Research*, pages 1188–1196, Beijing, China, 22–24 Jun 2014. PMLR. URL <http://proceedings.mlr.press/v32/le14.html>.
- Su-In Lee, Safiye Celik, Benjamin A Logsdon, Scott M Lundberg, Timothy J Martins, Vivian G Oehler, Elihu H Estey, Chris P Miller, Sylvia Chien, Jin Dai, et al. A machine learning approach to integrate big data for precision medicine in acute myeloid leukemia. *Nature communications*, 9(1):1–13, 2018.
- Li-Guan Li, Xiaole Yin, and Tong Zhang. Tracking antibiotic resistance gene pollution from different sources using machine-learning classification. *Microbiome*, 6(1):1–12, 2018.
- James L Maino, Paul A Umina, and Ary A Hoffmann. Climate contributes to the evolution of pesticide resistance. *Global Ecology and Biogeography*, 27(2):223–232, 2018.
- Ngoc Giang Nguyen, Vu Anh Tran, Duc Luu Ngo, Dau Phan, Favorisen Rosyking Lumbanraja, Mohammad Reza Faisal, Bahridin Abapihi, Mamoru Kubo, and Kenji Satou. DNA sequence classification by convolutional neural network. *JBiSE*, 09(05):280–286, 2016.
- F. Pedregosa, G. Varoquaux, A. Gramfort, V. Michel, B. Thirion, O. Grisel, M. Blondel, P. Prettenhofer, R. Weiss, V. Dubourg, J. Vanderplas, A. Passos, D. Cournapeau, M. Brucher, M. Perrot, and E. Duchesnay. Scikit-learn: Machine learning in Python. *Journal of Machine Learning Research*, 12:2825–2830, 2011.
- Grace C. Y. Peng, Mark Alber, Adrian Buganza Tepole, William R. Cannon, Suvranu De, Salvador Dura-Bernal, Krishna Garikipati, George Karniadakis, William W. Lytton, Paris Perdikaris, Linda Petzold, and Ellen Kuhl. Multiscale modeling meets machine learning: What can we learn? *Archives of Computational Methods in Engineering*, 2020.
- Mitchell W Pesesky, Tahir Hussain, Meghan Wallace, Sanket Patel, Saadia Andleeb, Carey-Ann D Burnham, and Gautam Dantas. Evaluation of machine learning and rules-based approaches for predicting antimicrobial resistance profiles in gram-negative bacilli from whole genome sequence data. *Frontiers in microbiology*, 7:1887, 2016.
- Sashank J. Reddi, Satyen Kale, and Sanjiv Kumar. On the convergence of adam and beyond. *arXiv*, (1904.09237), 2019.

- Burkhard Rost, Predrag Radivojac, and Yana Bromberg. Protein function in precision medicine: deep understanding with machine learning. *FEBS letters*, 590(15):2327–2341, 2016.
- Peter J. Rousseeuw. Silhouettes: A graphical aid to the interpretation and validation of cluster analysis. *Journal of Computational and Applied Mathematics*, 20:53 – 65, 1987. ISSN 0377-0427. doi: [https://doi.org/10.1016/0377-0427\(87\)90125-7](https://doi.org/10.1016/0377-0427(87)90125-7). URL <http://www.sciencedirect.com/science/article/pii/0377042787901257>.
- S Shadab, M T A Khan, N A Neezi, S Adilina, and others. DeepDBP: Deep neural networks for identification of DNA-binding proteins. *Informatics in Medicine*, 2020.
- Andrew E Teschendorff. Avoiding common pitfalls in machine learning omic data science. *Nature Materials*, 18(5):422–427, 2019.
- Ameni Trabelsi, Mohamed Chaabane, and Asa Ben-Hur. Comprehensive evaluation of deep learning architectures for prediction of DNA/RNA sequence binding specificities. *Bioinformatics*, 35(14):i269–i277, July 2019.
- Xin Yang and Tingwei Guo. Machine learning in plant disease research. *European Journal of BioMedical Research*, 3(1):6–9, 2017.
- Haoyang Zeng, Matthew D Edwards, Ge Liu, and David K Gifford. Convolutional neural network architectures for predicting DNA-protein binding. *Bioinformatics*, 32(12):i121–i127, June 2016.